Applied Catalysis A, General 619 (2021) 118124

Contents lists available at ScienceDirect

Applied Catalysis A, General

journal homepage: www.elsevier.com/locate/apcata

Highly dispersed Pd nanoparticles supported on γ-Al_2O_3 modified by minimal 3-aminopropyltriethoxysilane as effective catalysts for 2-ethyl-anthraquinone hydrogenation

Wenqian Li [a], Fuming Wang [a], Xubin Zhang [a,*], Mingshuai Sun [a], Jiaqi Hu [a], Yi Zhai [a], Huihui Lv [a], Guojun Lv [b]

[a] School of Chemical Engineering and Technology, Tianjin University, Tianjin 300350, PR China
[b] School of Environmental and Chemical Engineering, Jiangsu University of Science and Technology, Zhenjiang 212003, Jiangsu, PR China

ARTICLE INFO

Keywords:
Spherical γ-Al_2O_3
Anthraquinone hydrogenation
3-aminopropyltriethoxysilane
Supported Pd-based catalyst

ABSTRACT

Faced with the problems of poor activity and inferior selectivity, highly dispersed Pd catalysts pre-modified by minimal 3-aminopropyltriethoxysilane (APTES) were prepared via impregnation reduction method. The amount of APTES was adjusted according to molar ratios of the APTES to Pd (APTES/Pd). The catalytic hydrogenation efficiency exhibited a volcano-shape trend with the amount of APTES. Grafting of suitable amount of APTES improved the dispersion of the Pd, increased the weak acid content of the γ-Al_2O_3 and regulated the reducibility of the catalysts. The catalyst having APTES/Pd = 2 with 0.192 wt% Pd showed the highest catalytic activity and selectivity, with 100 % in the selectivity and the improvement of 27.3 % in the hydrogenation efficiency and 104.8 % in the H_2O_2 productivity compared with the commercial catalyst (0.298 wt%). Furthermore, the APTES aggregated with the amount of APTES, which provided intense anchoring sites for the Pd and resulted in the increase in larger palladium nanoparticles.

1. ntroduction

Hydrogen peroxide(H_2O_2)is widely applied in large-scale industrial fields due to its excellent oxidation performance and environmental friendly characteristics, such as detergent applications, chemical synthesis, paper bleaching and so on [1–3]. At present, the productivity of hydrogen peroxide manufactured by anthraquinone method accounts for more than 98 % of the scope of world [4]. In a typical auto-oxidation (AO)cycle (Scheme 1), 2-ethyl-anthraquinone is catalytically hydrogenated with H_2 to produce 2-ethylanthrahydroquinone ($EAQH_2$), $EAQH_2$ theoretically generates EAQ and the targeted H_2O_2 through rapid oxidation reaction. Nevertheless, the actual situation of the catalytically hydrogenation reaction accompanied by many side reactions. In the hydrogenation of EAQ, the produced $EAQH_2$ might go further deep hydrogenation to yield tetrahydro 2-ethylanthrahydroquinone (H_4EAQH_2) which can also be oxidized to form H_2O_2 and H_4EAQ, so EAQ and H_4EAQ are both called active anthraquinones and can be recycled in AO process. At the same time, the hydrogenation reaction will also produce other hydrogenation products through deep hydrogenation reaction, such as octahydro-2-ethylanthrahydroquinone (H_8EAQH_2), the other way can give 2-ethylanthrone (EAN) through hydrogenolysis of carbonyl bond, which is regarded as the main by-product. H_8EAQH_2 and EAN are entitled as degradation products because they cannot be used in the AO recycling process. The progressive increasing of degradation products could decrease the content of active anthraquinone in the working solution and negatively affect the catalytic performance of the catalyst, which would result in increasing the operating cost in the industrial process [5–8].

The palladium-based catalyst Pd/Al_2O_3 is widely applied in the industrial process of anthraquinone hydrogenation due to its excellent activity and stability [9,10]. Previous studies have proved that the anthraquinone hydrogenation was a fast reaction controlled by mass diffusion [11,12]. Now the problem faced of anthraquinone hydrogenation catalysts is to improve the selectivity and hydrogenation efficiency of the catalyst, which means that the investigation could be carried out from the perspective of improving the dispersion and electronic state of the metal palladium, as well as from the other perspective of advancing certain properties of the support. These desired

* Corresponding author.
E-mail address: tjzxb@tju.edu.cn (X. Zhang).

https://doi.org/10.1016/j.apcata.2021.118124
Received 20 January 2021; Received in revised form 7 March 2021; Accepted 27 March 2021
Available online 9 April 2021

achievements are mainly achieved by adding a second metal, doping heteroatoms and improving the structural properties, acidity, hydrophobic properties of the catalyst support and so on [13–17]. Yuan et al. prepared a series of bimetallic Pd-Co, Pd-Ag, and Pd-Cu catalysts and systematically studied the effect of the doping of the second metal on the catalytic hydrogenation performance of anthraquinone, found that the Pd-Co catalyst having Co/Pd = 0.25 prepared at a low reduction temperature of 80°C has the highest hydrogenation efficiency and selectivity and attributes it to the synergistic effect of the Pd-$M^{\alpha+}$ structure [18]. Feng et al. studied the influence of silica introduction on the improvement characteristic of the spherical SiO_2–Al_2O_3, found that catalytic performance of anthraquinone hydrogenation improved with increasing silica content [19]. Feng et al. prepared functionalized SBA-15 with alkyltriethoxysilane and found that the Pd catalyst supported functionalized with different alkyl group groups exhibited improved performance in the catalytic hydrogenation of 2-ethyl-anthraquinone, which could be attributed to the increase in hydrophobicity of SBA-15 and improvement of the absorption and diffusion of EAQ molecules [17]. Rodríguez-Gómez et al. found that the supported Au-Pd catalyst with functionalized SBA-15 which was modified by different organic groups (—SO_3H,$NH—_2$ and S—H) could improve catalytic activity in the direct synthesis of hydrogen peroxide reaction for a direct synthesis reaction [20].

The -NH_2 structural group in APTES could complex with metal palladium ions and act as an anchoring site for metal palladium. The addition of Si could adjust the acidity and basicity of alumina [19], and the alkyl groups are conducive to improving the hydrophobic properties of the catalyst [17]. The modification of γ-Al_2O_3 with APTES on the surface could take advantage of above possible way and almost no relevant investigations about the modification of APTES on the surface of spherical γ-Al_2O_3 for anthraquinone hydrogenation have been published. Therefore, catalyst Pd/γ-Al_2O_3 modified with APTES may be a potential candidate for anthraquinone hydrogenation.

In our work, a group of modified commercial γ-Al_2O_3 with different addition amount of APTES were synthesized for preparing the catalyst by the impregnation reduction method, and the hydrogenation performance of modified catalyst was investigated through 2-ethylanthraquinone hydrogenation. Herein, we explored the influence of modification of minimal APTES on the dispersion of the Pd, the size of the metal palladium nanoparticle, the weak acid content on the surface of the γ-Al_2O_3 and the reducibility of the catalyst, which were characterized by several analysis techniques including nitrogen adsorption-desorption, TEM, XRD, NH_3-TPD, XPS, H_2-O_2 titration, H_2-TPR, ICP-AES, TGA and elemental analysis.

2. Experimental section

2.1. Pre-modification of γ-Al_2O_3

The modification of γ-Al_2O_3 is to graft 3-aminopropyltriethoxysilane (Tianjin Heowns Biochem LLC, AR) to the surface of commercially available spherical alumina (Yantai Baichuan Huitong Technology Co. Ltd, China, grades 2.5−3 mm and surface area 171.58 m^2/g). The specific modified procedure of γ-Al_2O_3 is as follows. In a typical procedure, 5.0 g spherical alumina was refluxed in distilled water at 80 °C for 1 h to increase the content of surface hydroxyl groups, followed by filtration and drying overnight at 120 °C to yield rehydrated alumina [17]. Then a certain amount of APTES and 5.0 g rehydrated alumina was added to the 20 mL mixed solvent of 15 mL acetone (Damao Chemical Reagent Co. Ltd, China, AR) and 5 mL anhydrous ethanol (Kermel, China,AR) in sequence. The mixture was shook at 45 ℃ for 10 h, filtered and dried under vacuum overnight. The modified spherical alumina was named as γ-Al_2O_3-xAPTES-pre, where x represented the theoretical molar ratio of APTES to Pd in the support. The catalyst without APTES added was named γ-Al_2O_3-um, keeping the same preparation conditions as the above pre-modification method.

2.2. Preparation of Pd/γ-Al_2O_3 catalysts

The Pd-loaded catalyst was prepared by the incipient wetness impregnation. The acetone solution of $Pd(OAc)_2$ (Shanghai Dibo Chemical Technology Co. Ltd, China,) was prepared by dissolving 0.0106 g $Pd(OAc)_2$ in 20 mL acetone solution, then added 5 g of the modified spherical alumina to the above solution. The mixture was shook at 45 ℃ for 24 h in the shaker, dried under vacuum overnight. In our work, the theoretical metal mass loading of Pd/γ-Al_2O_3 catalyst was set to 0.2 wt%. Then the solid was calcined in air at 300 ℃ for 3 h with a ramping rate of 2.5 °C/min. Finally, all the samples were reduced by 10 vol% H_2/Ar at 180 °C for 3 h. The Pd catalysts were noted as 0.2 % Pd/γ-Al_2O_3-xAPTES-pre and 0.2 % Pd/γ-Al_2O_3-um.

At the same time, a post-grafting procedure was also used to prepare supported Pd-loaded catalyst. In this case, a certain amount of APTES was added to the mixed solution of $Pd(OAc)_2$ in acetone and anhydrous ethanol. Then the above mixture was stirred at 45 °C for 1 h and placed in a shaker at 45 °C for 24 h, subsequently dried, calcined and reduced under the same conditions as above 0.2 % Pd/γ-Al_2O_3-xAPTES-pre preparation procedure. The catalyst obtained by the post-grafting procedure method was named 0.2 % Pd/γ-Al_2O_3-xAPTES-post.

For comparison, the modified catalyst samples and the commercial catalyst (Yantai Baichuan Huitong Technology Co. Ltd, China, grades 2.5−3 mm, Pd mass loading 0.298 wt%) were ultimately tested in the heterogeneous hydrogenation of 2-alkylanthraquinone to investigate

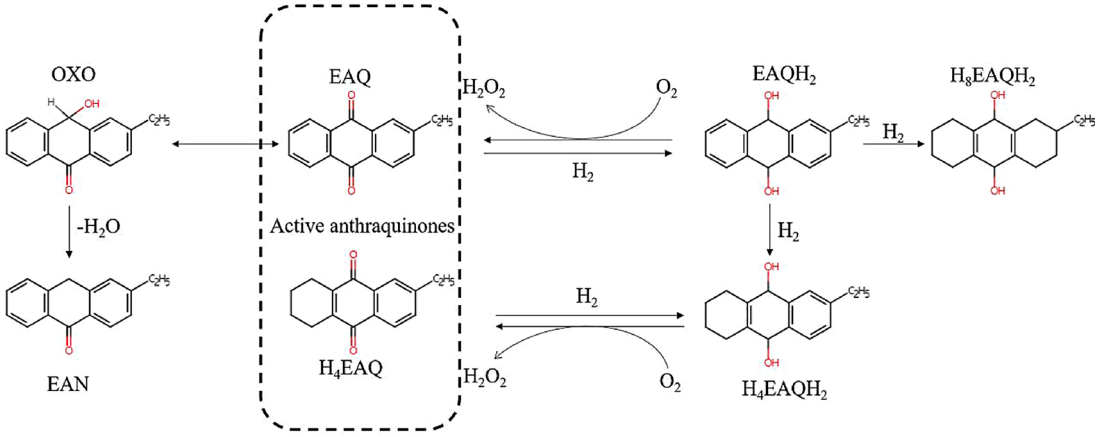

Scheme 1. Main reactions of anthraquinone hydrogenation process.

the difference in catalytic performance.

2.3. Analysis and characterization

The contents of the palladium and silicon in the catalysts were determined by an inductively coupled plasma atomic emission spectrometer (VISTA-MPX, Varian). The carbon and nitrogen contents were tested by elemental analysis on the CHN model Vario EL III of Elemental Analyses System. The thermogravimetric analysis (TGA, Labsys evo) was performed at nitrogen atmosphere from room temperature to 850 °C with a heating rate of 10 °C/min. In order to remove the physically adsorbed water in the sample, all samples to be tested need to be vacuum degassed at 200 ℃ for 3 h before TGA operating. Herein a high-resolution transmission electron microscope (HRTEM, JEM-2100 F, JEOL, Japan) were used to investigate the structure and particle size of catalysts. X-ray diffraction (XRD) patterns were recorded on D8-Focus diffractometer (Bruker Axs, Germany) equipped with a Cu radiation source (40 kV, 30 mA) in the 2θ range of 10–70° at a scan speed of 8°/min. The specific surface area and structural properties of the prepared catalysts were measured by nitrogen adsorption isotherms in SSA-7000 apparatus at the liquid nitrogen temperature. The pore size distribution was calculated according to the adsorption branch of isotherms based on BJH method. Before measurement operation, all the samples needed to be degassed under vacuum environment at 573 K for 2 h. X-ray photoelectron spectroscopy (XPS) was conducted on a Thermo Scientific ESCALAB 250Xi spectrometer equipped with an Al- Kα radiation source and using the C1 s peak as the internal standard (C1 s = 284.8 eV). Peak decomposition of XPS results were achieved using the XPSPEAK41 program with a Gaussian/Lorentzian function and a Shirley nonlinear sigmoid-type baseline. NH_3 temperature-programmed desorption (NH_3-TPD) of the samples was performed on an Auto Chem II 2920 chemisorption analyzer. About 0.3 g of the catalysts sample to be tested was put into a U-shaped quartz reactor and heated from room temperature to 300 ℃ at a temperature ramp rate of 10 °C/min under a high-purity He gas flow of 40 mL/min, and activate at constant temperature 300 ℃ for 2 h and then cooled down to 100 °C. NH_3 (20 vol% NH_3 in He) was introduced into the detection system and sample adsorbed NH_3 to saturation, then purged with helium until the baseline is stable. The adsorbed NH_3 of sample was gradually desorbed in He flow by raising the temperature from 100 ℃ to 600 ℃ at 10 ℃/min and a constant TCD signal was obtained.

For investigating the dispersion of metal palladium and the corresponding reducibility of the studied catalyst, H_2-O_2 titration and H_2-TPR were separately conducted on Auto Chem II 2910 analyzer with a thermal conductivity detector (TCD). For H_2-TPR, about 0.3 g sample was placed into a quartz reactor and pretreated in Ar flow at 150 ℃ for 1 h to remove water and impurity gas adsorbed on the sample. Then the sample was reduced in a 10 vol% H_2/Ar atmosphere with a flow rate of 40 mL/min at a rate of 10 ℃/min from 40 to 180°C. The specific operating steps of H_2-O_2 titration were as follows, about 0.3 g sample was placed in a quartz reactor with the Ar atmosphere at 180 °C for pretreatment for 2 h. After that, the sample with water and air removed was saturated with 10 vol% H_2/Ar at 180°C for 2 h and then sample was cooled to 100 °C. Next the carrier gas was switched to He gas for purging and after the baseline was stable, high purity oxygen was pulsed continuously until the peak area didn't change, meaning that oxygen saturation adsorption of the samples was achieved. The chemisorbed oxygen was then titrated by hydrogen in N_2 atmosphere until saturation adsorption hydrogen. The theoretical dispersion of Pd (D%) for the studied catalyst was deduced from the volume of H_2 adsorbed for the titration of O_2 as the following equation [21]:

$$D(\%) = \frac{2V_{H_2}M_{Pd}}{3 \times 22.4 w_{cat} m_{Pd}} \times 100$$

where V_{H_2} is volume of H_2 consumed (mL) for the titration of O_2, M_{Pd} is relative molecular mass of palladium, w_{cat} is operation used mass of sample catalyst in grams, and m_{Pd} is Pd loading concentration of each catalyst (wt%).

2.4. Catalytic performance tests

The hydrogenation experiments were carried out in an auto-clave reactor. The working solution was prepared by dissolving 120 g of solid 2-ethylanthraquinone (EAQ) in 1 L of a mixed solvent of trioctyl phosphate (TOP, 98 %, TCI) and trimethylbenzene (98 %, TCI) with the volume ratio of 1:1. All catalysts to be tested were completely reduced at 180 ℃ for 3 h in a tube furnace before hydrogenation reaction. In a typical run, 60 mL working solution and 1.2 g catalyst were sequentially put in the reactor which was maintained at a temperature of 60 ℃ and a hydrogen pressure of 0.3 MPa with a rotating speed of 800 r/min. When the hydrogenation reaction proceeds to a certain time, 2 mL of the hydrogenated product was taken out for analysis in the process of the hydrogenation reaction. Then, the catalyst-free hydrogenated solution was placed into 20 mL of deionized water and sufficiently oxygenized by O_2 at 30 ℃ for 30 min in a separating funnel. After the oxidation reaction, a H_2O_2 aqueous solution was extracted three times with distilled water and the water-phase was titrated by $KMnO_4$ solution to determine the H_2O_2 content. The catalytic activity is expressed as follow equation [22]:

$$B = \frac{5}{2}\frac{C \times V_0 \times M}{V}$$

where B is the hydrogenation efficiency (g/L), which is meaning of the mass of H_2O_2 formed per volume working solution, C is concentration of $KMnO_4$ solution (mol/L), V_0 is the volume of $KMnO_4$ solution used during the titration (mL), V is the volume of H_2O_2 solution (mL), and M is the molar mass of H_2O_2 (g/mol). The productivity of H_2O_2 can be expressed by the following equations:

$$H_2O_2 \text{ productivity} = m(g,\ H_2O_2)/[m(g,\ Pd)\cdot h]$$

A high performance liquid chromatograph (HPLC, Prominence-i LC-2030) equipped with a Durashell C18 (5 um, 4.6 × 250 mm) separation column and UV detector was taken as serve to analyze the concentrations of EAQ and H_4EAQ, which were respectively denoted as $n_{t(EAQ)}$ and $n_{t(H_4EAQ)}$, and the initial concentration of EAQ was denoted as $n_{0(EAQ)}$.The mobile phase was a mixture of methanol and ultra-pure water with a volume ratio of 80 : 20. The wavelength of the ultraviolet radiation was 245 nm. The catalyst selectivity is defined as following equations:

$$S = \frac{n_{t(EAQ)} + n_{t(H_4EAQ)}}{n_{0(EAQ)}} \times 100\%$$

The number of exposed active sites (N_{Pd}) can be expressed by the following equations:

$$N_{Pd} = \frac{m_{Pd} \times w_{cat} \times D\%}{M_{Pd}} \times N_A$$

Where m_{Pd} is Pd loading concentration of each catalyst (wt%), w_{cat} is operation used mass of sample catalyst in grams, D% is the theoretical dispersion of Pd by H_2-O_2 titration, M_{Pd} is relative molecular mass of palladium and N_A is the Avogadro constant.

The hydroxyl density on the surface of γ-Al_2O_3 could be calculated by the following equations:

$$m_{OH} = \frac{m_{T=473.15K} - m_{T=973.15k}}{M_{H_2O} \times m_s}$$

Where m_{OH} is hydroxyl density on Al_2O_3 surface each sample (mmol/g), $m_{T=473.15K}$ is the mass of the sample measured at T = 473.15 K by TGA. $m_{T=973.15k}$ is the mass of the sample measured at T = 973.15 K by TGA. M_{H_2O} is relative molecular mass of H_2O. m_s is the mass of the sample used in the TGA measurement.

3. Results and discussion

3.1. Characterization of prepared catalysts

Palladium nanoparticles size distribution is analyzed by TEM technology and corresponding images are displayed in Fig. 1, in which black spots are attributed to palladium nanoparticles. As can be seen from the above patterns, the palladium nanoparticles size of the modified catalyst (ca.1.76 nm–2.11 nm) is smaller than the unmodified catalyst 0.2 % Pd/γ-Al_2O_3-um (2.59 nm), suggesting that the grafting of APTES on surface of the γ-Al_2O_3 could reduce the size of the metal palladium nanoparticle and inhibit its agglomeration. For catalyst 0.2 % Pd/γ-Al_2O_3-2APTES-Pre, it can be observed that the palladium crystal particle size is restricted to a small narrow range within 2.40 nm, which dominate the size distribution with more than 94 %. For catalyst 0.2 % Pd/γ-Al_2O_3-1APTES-Pre with a lower APTES content, the palladium crystal size has a wider size distribution (1.2–5.5 nm) and a larger average particle size (1.97 nm) compared with 0.2 % Pd/γ-Al_2O_3-2APTES-Pre. Also for catalysts 0.2 % Pd/γ-Al_2O_3-xAPTES-Pre (x = 4,8), the palladium crystalline size is also mostly smaller than 2.4 nm, but the proportion in the range of 2.4–6.0 nm is gradually increasing from 5.94 % to 14.85 % and slightly larger average particle diameters are counted to be 1.91 nm and 2.11 nm, respectively. In the meantime, it could still be observed from Fig. 1 that the number of larger palladium particles with a size of 4–6.25 nm increases significantly for modified catalysts with the increase in the amount of APTES. In summary, the palladium crystal size exhibits a volcano-shape trend with the addition of APTES, which can be well consistent with the results of H_2-O_2 titration and H_2-TPR. Furthermore, these results give direct evidence that the increase in the content of APTES would intensify the agglomeration of metal palladium and lead to a decrease in metal dispersion.

The Pd loading and silicon content on the γ-Al_2O_3 is obtained by ICP-AES in Table 1, the actual Pd loading amount is close to the theoretical values of addition (0.2 wt%) and the Pd loading Pd/γ-Al_2O_3-xAPTES (x = 1, 2, 4, 8) is approximately 66.7 % of commercial catalyst (0.298 wt %). The silicon content at Pd/APTES = 1 is close to the theoretical addition but is getting smaller and smaller than the theoretical addition with increase in Pd/APTES, which is consistent with the elemental analysis results of carbon and nitrogen content. In order to quantitatively determine that APTES is successfully grafted on the γ-Al_2O_3 surface, the carbon and nitrogen contents of all pre-modified catalysts are measured by elemental analysis. The contents of C (0.74 wt‰) and N (0.07 wt‰) are an approximation of the theoretical added value for the Pd/APTES = 1 from the Table 1. Furthermore, the carbon and nitrogen contents of catalysts 0.2 % Pd/γ-Al_2O_3-xAPTES-Pre (x = 1,2,4,8) show an increasing trend with a multiplied increase in the value of Pd/APTES, but the deviation between the above results and the theoretical value of APTES is getting bigger and bigger. This remarkable phenomenon may be attributed to the limited grafting amount of APTES on the surface of γ-Al_2O_3 and a certain amount of APTES remained on the bottle wall during the pre-modified process.

Fig. 2 shows the powder XRD patterns of the prepared samples in which the effects of the APTES addition on the crystalline structure of the sample was explored. The peaks located at around 2θ = 36.5°, 39.5°,

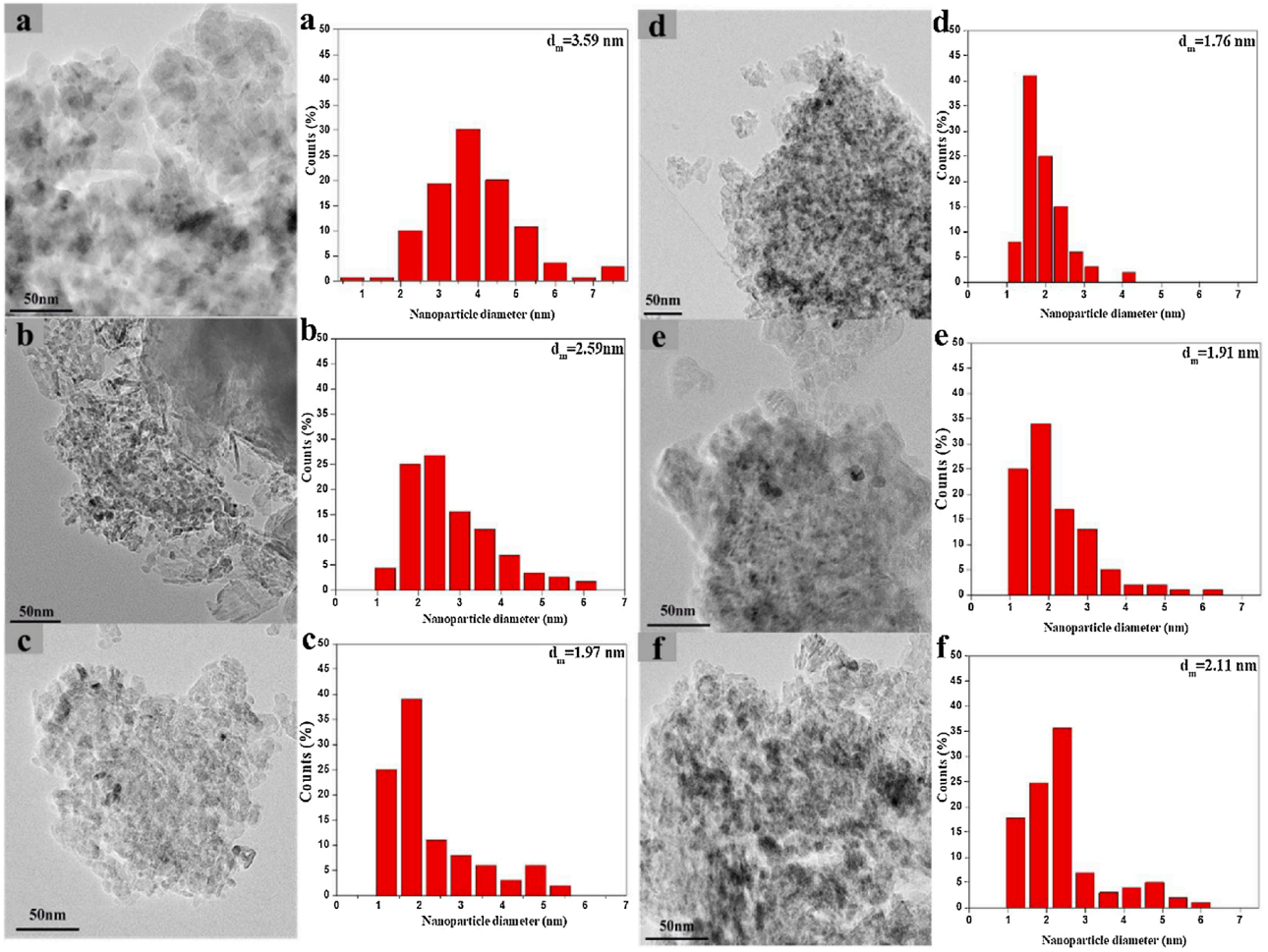

Fig. 1. TEM images and the size distribution of Pd particles in studied catalysts. (a) 0.3 % Pd/γ-Al_2O_3–Commercial, (b) 0.2 % Pd/γ-Al_2O_3-um, (c) 0.2 % Pd/γ-Al_2O_3-1APTES-Pre, (d) 0.2 % Pd/γ-Al_2O_3-2APTES-Pre, (e) 0.2 % Pd/γ-Al_2O_3-4APTES-Pre and (f) 0.2 % Pd/γ-Al_2O_3-8APTES-Pre.

Table 1
Physicochemical Characteristic and Metal Concentration of the Studied Samples.

Sample	Pd[a] (wt.‰)	Si[a] (wt.‰)	C[e] (wt.‰)	N[e] (wt.‰)	D[c] (%)	S_{BET}[b] (m^2g^{-1})	D_p[b] (nm)	pore volume ($cm^3\ g^{-1}$)	d_{TEM}[d] (nm)
γ-Al_2O_3-Commercial	——	——	——	——	——	171.58	4.66	0.530	——
0.3 % Pd/γ-Al_2O_3-Commercial	2.98	——	——	——	28	——	——	——	3.59
0.2 % Pd/γ-Al_2O_3-um	1.89	——	——	——	41	164.28	4.48	0.551	2.59
0.2 % Pd/γ-Al_2O_3-1APTES-Pre	1.90	0.50	0.74	0.07	50	150.49	4.62	0.566	1.97
0.2 % Pd/γ-Al_2O_3-2APTES-Pre	1.92	0.80	1.05	0.14	63	149.12	4.92	0.481	1.76
0.2 % Pd/γ-Al_2O_3-4APTES-Pre	1.88	1.18	1.37	0.22	61	148.44	5.17	0.508	1.91
0.2 % Pd/γ-Al_2O_3-8APTES-Pre	1.93	1.69	1.72	0.31	49	148.23	5.55	0.554	2.11

[a] Pd loading determined by ICP-AES analysis.
[b] Structural information determined by BET method.
[c] Pd dispersion determined by H_2-O_2 titration.
[d] Size of Pd particle obtained by TEM.
[e] Carbon and nitrogen content of catalysts determined by elemental analysis.

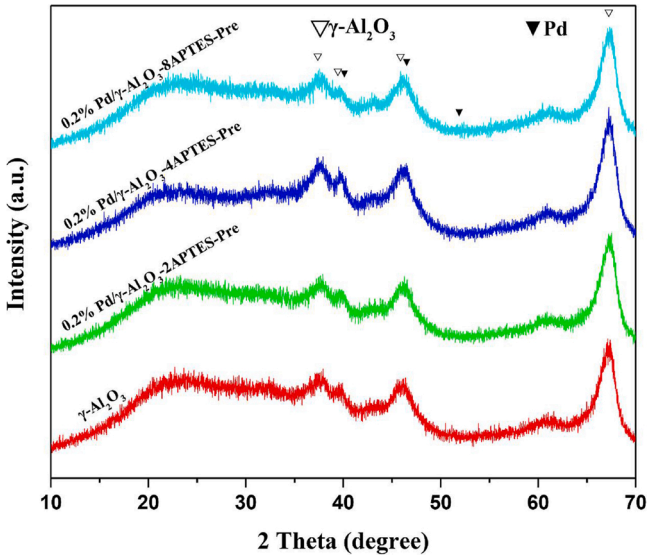

Fig. 2. XRD patterns of the studied samples.

45.8° and 67.0° are attributed to the (3 1 1), (2 2 2), (4 0 0) and (4 4 0) crystal faces of γ-Al_2O_3 phase (JCPDS Card No.10-0425) [23]. Meanwhile, no obvious diffraction peaks of palladium were detected at 2θ = 40.1°, 46.5°, and 51.9°, attributed to the (1 1 1), (2 0 0), and (4 2 2) crystal faces of palladium (JCPDS Card No.46-1043 and 011310, respectively) [24]. This may be caused by the low metal palladium loading and the high dispersion of metal palladium on γ-Al_2O_3.

In order to analyze the Pd metal dispersion more accurately, H_2-O_2 titration technique was implemented and the corresponding results are summarized in Table 1. From the result data of H_2-O_2 titrations, it can be seen that the metal dispersion in the 0.2 % Pd/γ-Al_2O_3-2APTES catalysts (63 %) was almost twice than that of the 0.3 % Pd/γ-Al_2O_3-Commercial catalyst (28 %) and other modified catalysts 0.2 % Pd/γ-Al_2O_4-xAPTES (x = 1, 4, 8) also had a higher degree of metal dispersion than the unmodified catalyst 0.2 % Pd/γ-Al_2O_3-um (41 %). At the same time, the metal dispersion is corresponding decreasing with the increase of the amount of APTES. On the one hand, the metal dispersion of the modified catalyst could be well improved compared with 0.2 % Pd/γ-Al_2O_3-um. On the other hand, excessive addition of APTES will aggravate the agglomeration of the metal palladium and cause the decrease of the metal dispersion. This phenomenon was consistence with H_2-TPR and TEM results, and the uniformly dispersed palladium with smaller particle sizes would lead to more conducive to catalytic performance for the hydrogenation of 2-alkylanthraquinone.

XPS measurements were conducted to further explore the electronic effect of the APTES modification on the electronic structure of the catalyst and the corresponding XPS photoelectron spectra in the N 1s, Si 2p and Pd 3d level of reduced catalysts are shown in Fig. 3. Fig. 3(A) shows the obtained Pd 3d spectra of Pd/γ-Al_2O_3-xAPTES and Pd/γ-Al_2O_3 catalysts. The binding energies of 335.1 eV and 340.4 eV could be assigned to Pd° $3d_{5/2}$ and Pd° $3d_{3/2}$. The other peaks at 336.1 eV and 341.4 eV belong to Pd $3d_{5/2}$ and Pd $3d3_{3/2}$ corresponding to Pd^{2+} [25, 26]. The binding energies and proportion of valence states of oxidized and reduced palladium states are summarized in Table 2. It is worth noting that the ratio of Pd°/Pd^{2+} increases due to APTES incorporation compared with Pd/γ-Al_2O_3-um catalyst, indicating that the modification of APTES could improve the reduction of the palladium precursor. In anthraquinone hydrogenation reaction, the increase of Pd°/Pd^{2+} ratio means that a greater proportion of reduced palladium states existed on the surface of the catalyst could be formed under the same reducing conditions, which would improve the hydrogenation efficiency [27].

For Si 2p XPS spectra (Fig. 2C), the binding energies (BE) of the sub-peaks at 98.6 eV, 100.4 eV and 101.8 eV corresponded to the Si°, Si-C and Si-O groups [28]. It is striking that the peak intensity at 101.8 eV continues to increase while the peak position shifts slightly toward higher BE (ca. 0.2 eV) with the increasing of the amount of APTES. This result suggests that excessive addition of APTES will increase the content of Si-O state and move to the high valence state, which is mainly caused by the hydrolysis and condensation between APTES and macromolecular compounds. In addition, the N 1s XPS spectra of the samples could be divided into two sub-peaks, which are set to be at 398.9 eV and 400.8 eV corresponding to the —NH_2 bonds and NC— bonds species, respectively [29–31]. It is observed that the BE of N 1s both sub-peaks shift toward higher BE with increasing of APTES content, this may be caused by the formation of a C-N-O bond between the oxygen element in γ-Al_2O_3 and the N element in APTES during the modification process.

H_2-TPR analysis test was conducted to investigate the reducibility of 0.2 % Pd/γ-Al_2O_3-um and 0.2 % Pd/γ-Al_2O_3-xAPTES (x = 1, 2, 8), and corresponding reduction results curves are presented in Fig. 4. As can be seen from the pattern, only one main reduction peak of all samples at ca. 77°C is observed which is attributed to the reduction of highly dispersed PdO species on the surface of the catalysts [32]. As reported in the literature, the main peak make at 77°C makes the most contribution to catalytic hydrogenation of 2-EAQ as the active site to adsorb hydrogen [33]. The reduction peak temperature for Pd/γ-Al_2O_3-xAPTES exhibits a volcano-shape trend of increasing first and then decreasing with the increase in the amount of APTES. In addition, the reduction peak temperature of catalyst 0.2 % Pd/γ-Al_2O_3-2APTES-Pre is the lowest among all modified catalysts, which is about 2.5 °C lower than that of catalyst 0.2 % Pd/γ-Al_2O_3-um. This peculiar phenomenon implies that the reduction peak temperature of the modified catalysts decreases due to the slight increase in the size of PdO crystals and the slight decrease in the dispersion of the palladium metal on the surface of the catalysts, which can be well correlated with the results of the TEM and H_2-O_2 titration results.

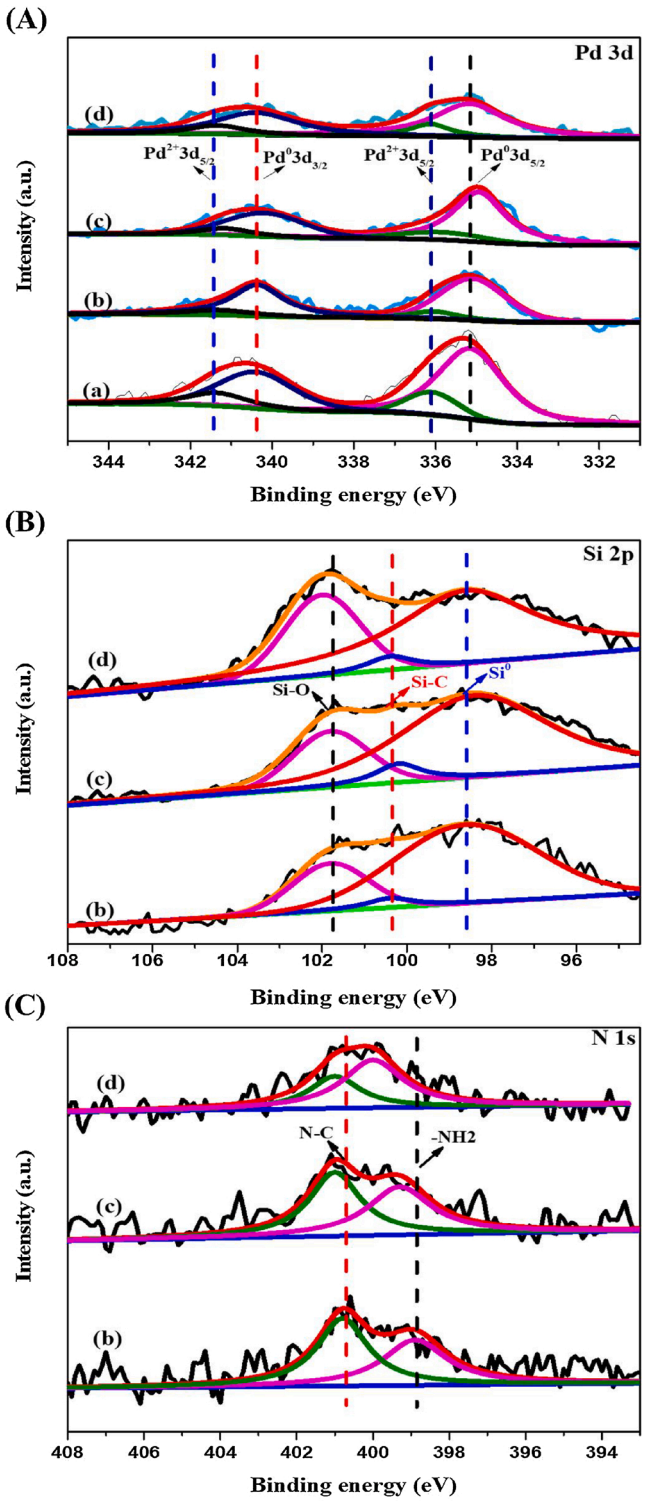

Fig. 3. (A) Pd 3d, (B) Si 2p and (C) N 1s spectra of reduced catalysts. (a) 0.2 % Pd/γ-Al_2O_3-um, (b) 0.2 % Pd/γ-Al_2O_3-2APTES-Pre and (c) 0.2 % Pd/γ-Al_2O_3-4APTES-Pre, (d) 0.2 % Pd/γ-Al_2O_3-8APTES-Pre.

Table 2
The peak position and proportion of valence states of Pd 3d.

Sample	$3d_{5/2}$ BE (eV)			$3d_{3/2}$ BE (eV)		
	Pd^0	Pd^{2+}	Pd^0/ Pd^{2+}	Pd^0	Pd^{2+}	Pd^0/ Pd^{2+}
0.2 % Pd/γ-Al_2O_3-um	335.1	336.1	4.4	340.4	341.4	3.2
0.2 % Pd/γ-Al_2O_3-2APTES-Pre	335.1	336.1	5.4	340.4	341.4	5.9
0.2 % Pd/γ-Al_2O_3-4APTES-Pre	334.9	335.9	4.4	340.2	341.2	4.3
0.2 % Pd/γ-Al_2O_3-8APTES-Pre	335.2	336.2	5.3	340.5	341.5	5.1

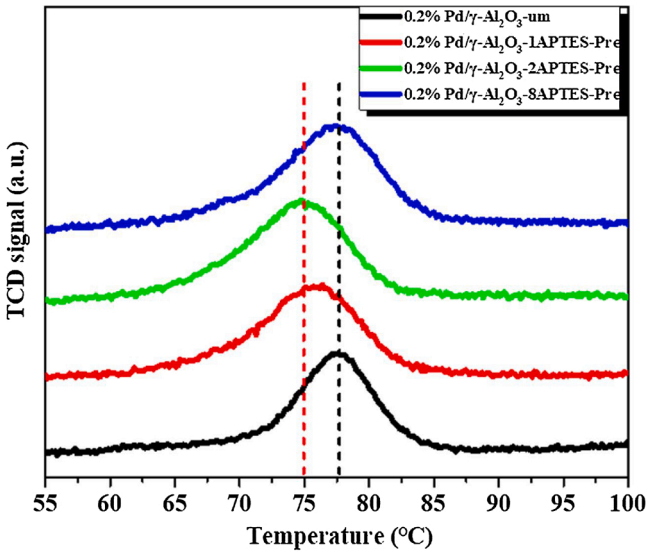

Fig. 4. H_2-TPR profiles of the prepared samples.

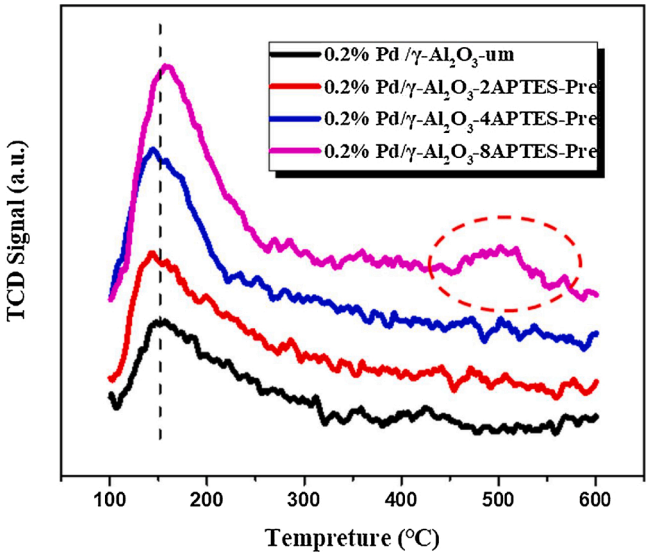

Fig. 5. NH_3-TPD profiles of the prepared samples.

The acidic properties of Pd/γ-Al_2O_3-um and Pd/γ-Al_2O_3-xAPTES with different APTES contents were evaluated using the NH_3-TPD technique and the corresponding profiles are shown in Fig. 5. Each curve shows typically single peak with a strong peak intensity centered around 157°C attributed to weak acid sites and one or more extremely weak peak between 400°C and 550°C attributed to strong acid sites. This situation leads to the assumption that the mainly one type of acid sites exist on the surface of the catalysts. But strong acid content is not summarized in the Table 2 because the peak intensity is too weak [34]. The acid properties of related catalysts are listed in Table 3. From the Fig. 5 and Table 3, it can be seen that the content of weak acid sites represented by the area of the lower temperature peak gradually increases with the increase of the content of APTES. The result is in

Table 3
Acid amount of the catalysts with different content of APTES.

Sample	Weak acid site	
	Temperature °C	Acid amount mmol/g
0.2 % Pd/γ-Al_2O_3-um	157.16	0.0226
0.2 % Pd/γ-Al_2O_3-2APTES-Pre	155.37	0.0235
0.2 % Pd/γ-Al_2O_3-4APTES-Pre	159.62	0.0287
0.2 % Pd/γ-Al_2O_3-8APTES-Pre	158.68	0.0440

accordance with the investigation by Feng et al. [19], which could be ascribed to the Si—OH group on the surface of modified catalyst. In addition, a faint peak at about 500 ℃ appeared for Pd/γ-Al_2O_3-8APTES-pre, suggesting the appearance of weak strong acid sites.

TG curves of studied γ-Al_2O_3 samples and corresponding hydroxyl density m_{OH} on alumina surface are displayed in Fig. 9. The mass loss of samples within 200℃ could be regarded as caused by the desorption of physically adsorbed water. Therefore, we choose the mass loss that occurs in the 200°C–700°C range as the basis for calculating the hydroxyl density. As can be seen from the Fig. 6 and results of m_{OH}, the content of surface hydroxyl groups can be greatly increased through hydration from 1.09 mmol/g of hydrated γ-Al_2O_3 to 2.30 mmol/g of unhydrated γ-Al_2O_3, which is beneficial to the grafting of APTES on the surface of alumina.

The nitrogen adsorption-desorption isotherms and pore size distributions of four samples are shown in Fig. 7. The corresponding textural properties including specific surface area (S_{BET}), total pore volume and average pore size (D_p) are summarized in Table 1. As shown in Fig. 7a, all the samples display typical type IV isotherms with distinct H3 hysteresis loops at relative pressure $P/P_0 > 0.7$ attributed to capillary condensation, revealing their mesoporous properties [23]. Meanwhile, it can be seen that and the pore size distributions of all samples exhibit single peak and the most pore size is concentrated around 10.0 nm and the effect of addition of APTES on the textual properties of catalyst is negligible. However, the specific surface areas of Pd/γ-Al_2O_3-xAPTES are slightly lower than γ-Al_2O_3 indicating that the loading of palladium and the grafting of APTES would occupy part of the tunnel. Furthermore, the average pore size of modified catalysts gradually increases with the increase of the addition of APTES and this peculiar result is attributed to the fact that APTES would preferentially clog smaller pores. This would cause the modification of APTES is uneven on the surface of γ-Al_2O_3 and then results in uneven particle size distribution of palladium metal, which is consistence with the results of H_2-O_2 titration data and the TEM.

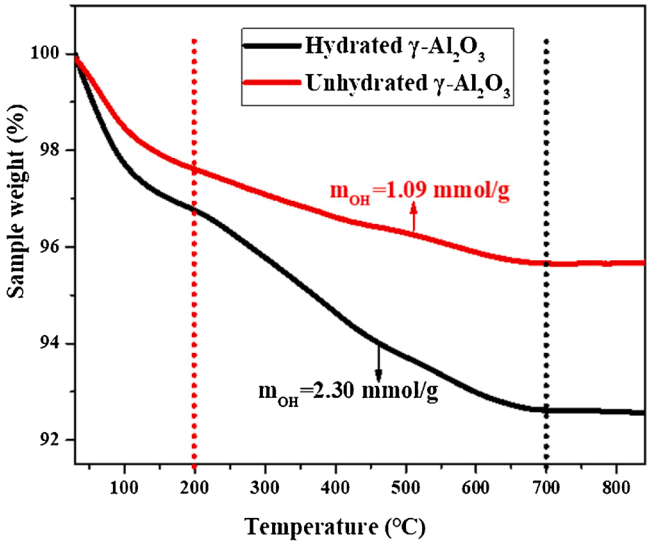

Fig. 6. TG analysis of hydrated γ-Al_2O_3 and unhydrated γ-Al_2O_3.

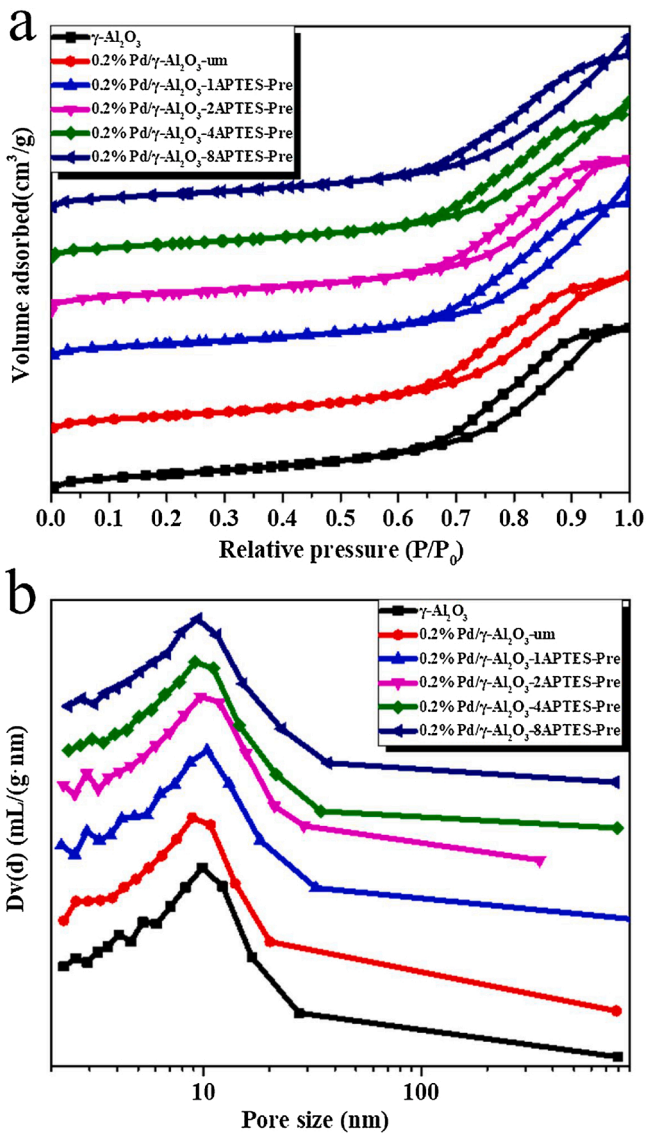

Fig. 7. a Nitrogen adsorption-desorption isotherms and b the pore size distributions of the samples.

3.2. Catalytic performance

In order to verify the effect of modification of APTES on the anthraquinone hydrogenation performance of the catalyst, a series of hydrogenation reaction experiments of 2-EAQ were performed in the agitated auto-clave reactor. First of all, the Pd-based catalyst 0.2 % Pd/γ-Al_2O_3-xAPTES-pre (x = 1, 2, 4, 8) and 0.2 % Pd/γ-Al_2O_3-2APTES-post were prepared. The hydrogenation efficiency of the catalyst increases from 11.57 g/L to 12.84 g/L with the increase of the molar ratio of APTES/Pd in the Fig. 8a. The hydrogenation efficiency of all modified catalysts with APTES are higher than that of unmodified catalysts (7.69 g/L,). 0.2 % Pd/γ-Al_2O_3-2APTES-pre catalyst displays the maximum activity, which is 1.67 times higher than that of the unmodified catalyst. Then, we used the post-modification method to prepare 0.2 % Pd/γ-Al_2O_3-2APTES-post to explore the effect of the modification sequence on the hydrogenation activity of the catalyst. It was observed that the catalyst obtained by the post-modification method had much lower hydrogenation activity than the pre-modification method. In summary, it can be concluded that the modification of APTES could greatly

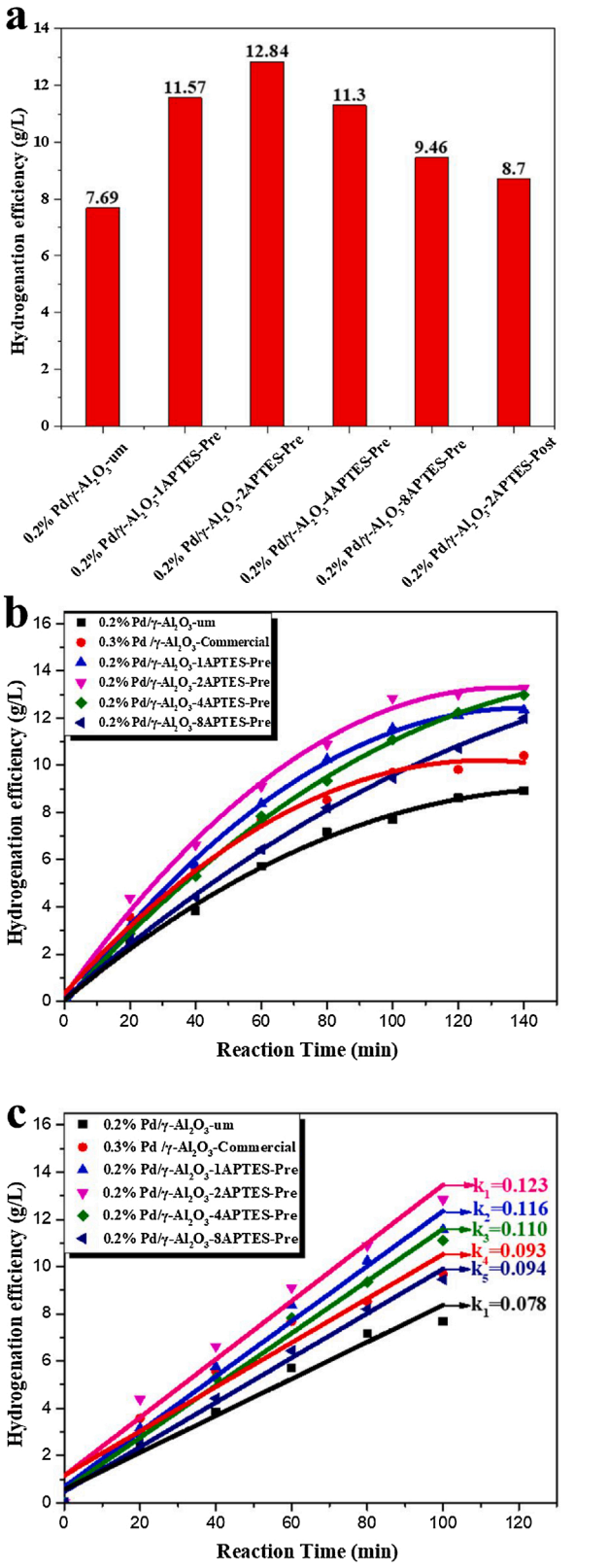

Fig. 8. Results of anthraquinone hydrogenation over studied catalysts (a) Hydrogenation performance of the studied catalyst at a reaction time of 100 min, (b) Hydrogenation efficiency as a function of reaction time and (c) the linear fitting of hydrogenation efficiency and reaction time within 100 min (reaction conditions: catalyst: 1.20 g, temperature: 60 °C, H_2 pressure: 0.3 MPa).

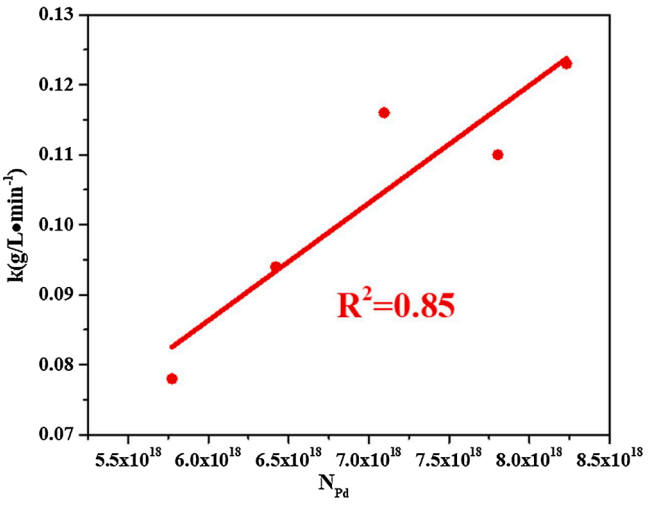

Fig. 9. Hydrogenation rate k as a function of exposed active sites N_{Pd}.

improve the hydrogenation activity of the catalyst. Moreover, the linear fitting of hydrogenation efficiency and reaction time is done within 100 min, and the slope of the curve is defined as the hydrogen efficiency rate k (g/L min^{-1}).

From the results of catalytic hydrogenation efficiency curves of Fig. 8b, hydrogenation reaction is characterized by the 2-EAQ to form 2-$EAQH_2$ at the initial stage of the hydrogenation corresponding to about 0~85 min. During the reaction stage, the hydrogen efficiency performance increases almost linearly and the hydrogenation rate is much faster than the subsequent hydrogenation reaction because the hydrogenation reaction network enters into the deep hydrogenation stage after about 85 min [24,35]. The hydrogen efficiency of catalyst Pd/γ-Al_2O_3-2APTES-pre could reach 13.26 g/L at 140 min, which is 27.3 % higher than that of the commercial catalyst (10.42 g/L). In the meantime, the hydrogen efficiency rate k increases from 0.078 g/L min^{-1} of the 0.2 % Pd/γ-Al_2O_3-um to 0.123 g/L min^{-1} of the 0.2 % Pd/γ-Al_2O_3-2APTES-pre catalyst in Fig. 8c, suggesting that a minimal modification of APTES can greatly improve the hydrogenation rate. However, as shown in Fig. 8a, it can be seen that the hydrogenation efficiency of the catalyst at 100 min ranges from 12.84 g/L (Pd/γ-Al_2O_3-2APTES-pre), 11.30 g/L (Pd/γ-Al_2O_3-4APTES-pre) to 9.46 g/L (Pd/γ-Al_2O_3-8APTES-pre) as the modification amount of APTES increases, indicating there is an optimal value for the added content of APTES to improve the hydrogenation activity of -nthraquinone.

Respect to the selectivity and H_2O_2 productivity, it can be seen from

Table 4
Hydrogenation performance of catalyst.

Sample	Hydrogenation efficiency (g/L)[a]	H_2O_2 productivity (g H_2O_2 g^{-1} Pd h^{-1})[a]	Selectivity (%)[b]
Pd/γ-Al_2O_3-Commercial	9.71	1629.38	96.96
0.2 % Pd/γ-Al_2O_3-um	7.69	2034.39	98.24
0.2 % Pd/γ-Al_2O_3-1APTES-Pre	11.57	3044.74	99.10
0.2 % Pd/γ-Al_2O_3-2APTES-Pre	12.84	3336.73	100
0.2 % Pd/γ-Al_2O_3-4APTES-Pre	11.30	2999.91	100
0.2 % Pd/γ-Al_2O_3-8APTES-Pre	9.46	2452.03	98.88

Reaction conditions: Working solution dosage:60 mL. Addition amount of catalyst:1.2 g. Temperature:60°C. Pressure:0.3 MPa.

[a] Reaction Time:100 min.

[b] Reaction Time:140 min.

Table 4 that H_2O_2 productivity of all modification catalysts has been significantly improved relative to commercial catalyst and unmodified catalyst, among which the Pd/γ-Al_2O_3-2APTES-pre with the best activity can be up to 2.05 times than commercial catalyst and 1.64 times than unmodified catalyst. The selectivity of the catalyst increased from 98.24 % of 0.2 % Pd/γ-Al_2O_3-um to 100 % of Pd/γ-Al_2O_3-2APTES-pre catalyst and significantly higher than commercial catalysts (96.96 %). Furthermore, both selectivity and H_2O_2 productivity typically exhibit exhibited a volcano-shape trend with the increase of the amount of APTES. These results could be well consistent with the anthraquinone hydrogen efficiency results.

According to the discussion of H_2—O_2 titration, TEM, XPS and H_2-TPR the modification of minimal APTES could greatly improve the dispersion of the Pd, reduce the size of the metal palladium nanoparticle, regulate the reducibility of the catalysts, which would provide more active sites for the anthraquinone hydrogenation reaction. However, the agglomeration of palladium is further increased and the dispersion of palladium is decreased as the amount of APTES added increases. The results of these characterizations successfully explain the performance of prepared catalysts for anthraquinone hydrogenation. In addition, it can be obtained from the Fig. 9 that the hydrogenation rate k has a good linear relationship (linear coefficient $R^2 = 0.85$) with the number of exposed active sites (N_{Pd}), which well illustrates that dispersion of Pd is the main factor in improving anthraquinone hydrogenation activity. Combining the BET results, XPS results and elemental analysis, the modification of APTES could block the smaller pores and decrease the impregnation depth of Pd, and the C—C group could improve the hydrophobicity of the γ-Al_2O_3. Related reports have confirmed that the lipophilicity of the catalyst could facilitate the desorption of $EAOH_2$ on the surface of γ-Al_2O_3 and hinder the deep hydrogenation [17,36]. Increase in average pore sizes could also effectively lower the diffusion resistance of EAQ in the catalytic hydrogenation. Therefore, the selectivity of the modified catalysts is significantly improved. However, the selectivity of Pd/γ-Al_2O_3-8APTES-pre decreases slightly from Table 4. As discussed in NH_3-TPD result, Pd/γ-Al_2O_3-8APTES-pre has the highest content of weak acid sites and weak strong acid site signals. According to the previous reports, the acidic sites on the surface of catalysts participate in the hydrogenation by acting as adsorption sites for EAQ molecules and EAQ adsorbed on the strong acid sites is more conducive to side reactions and produce more by-products [16,19,35]. This may be the cause of poor selectivity for Pd/γ-Al_2O_3-8APTES-pre.

4. Conclusion

In this work, a group of catalysts modified with different amounts of APTES were prepared by the impregnation method and evaluated through the EAQ hydrogenation reaction. It was found that Pd/γ-Al_2O_3-2APTES-pre with a metal loading of 0.192 wt% showed the highest catalytic activity and selectivity among all modified catalysts. Combining the results of the characterization analysis and the hydrogenation performance evaluation of the studied catalysts clearly demonstrated that the modification of suitable amount of APTES greatly improved the dispersion of the Pd, reduced the size of the metal palladium nanoparticle, improved the hydrophobicity, increased the weak acid content on the surface of the γ-Al_2O_3 and regulated the reducibility of the catalysts. These characteristics are beneficial to the advanced catalytic performance of supported palladium-based catalyst in the EAQ hydrogenation. But when the modification amount of APTES increases in excessive molar multiples, the metal dispersion of catalyst decreased and clusters of larger palladium nanoparticle begun to increase. This is due to the group dendritic structure with -NH_2 of APTES acts as moderate anchoring sites of palladium precursor. However, APTES would aggregate with greater probability as the amount increases on the surface of γ-Al_2O_3, which could provide more concentrated and intense anchoring for the metal palladium and result in the increase in size of larger palladium nanoparticles and a decrease in metal dispersion. Furthermore, the modification amount of APTES (0.038 μmol/g ~ 0.15 μmol/g) is minimal and the modification steps are extremely simple, so it is expected to decrease precious metal content of catalyst in industrial application.

CRediT authorship contribution statement

Wenqian Li: Experiment, Conceptualization, Methodology, Formal analysis, Investigation, Writing-Original Draft. **Fumin Wang:** Conceptualization, Supervision, Writing-Review & Editing. **Xubin Zhang:** Conceptualization, Methodology, Supervision. **Mingshuai Sun:** Conceptualization, Data Curation, Supervision. **Jiaqi Hu:** Validation, Data Curation, Formal analysis. **Yi Zhai:** Validation, Data Curation, Formal analysis. **Huihui Lv:** Validation, Data Curation. **Guojun Lv:** Validation, Data Curation.

Declaration of Competing Interest

The authors declare that they have no known competing financial interests or personal relationships that could have appeared to influence the work reported in this paper.

Acknowledgement

This work was supported by the National Natural Science Foundation of China (Grant No: 21978198, 22002052).

References

[1] J.M. Campos-Martin, G. Blanco-Brieva, J.L. Fierro, Angew. Chem. Int. Ed. Engl. 45 (2006) 6962–6984.
[2] R. Ciriminna, L. Albanese, F. Meneguzzo, M. Pagliaro, ChemSusChem 9 (2016) 3374–3381.
[3] R. Guan, X. Yuan, Z. Wu, L. Jiang, Y. Li, G. Zeng, Chem. Eng. J. 339 (2018) 519–530.
[4] Y. Guo, C. Dai, Z. Lei, Chem. Eng. Process. 136 (2019) 211–225.
[5] R. Kosydar, A. Drelinkiewicz, J.P. Ganhy, Catal. Lett. 139 (2010) 105–113.
[6] A. Drelinkiewicz, A. Waksmundzka-Góra, J. Mol. Catal. A Chem. 246 (2006) 167–175.
[7] A. Drelinkiewicz, J. Mol. Catal. A Chem. 101 (1995) 61–74.
[8] Q. Chen, Chem. Eng. Process. 47 (2008) 787–792.
[9] A. Drelinkiewicz, M. Hasik, M. Kloc, J. Catal. 186 (1999) 123–133.
[10] C. Shen, Y.J. Wang, J.H. Xu, Y.C. Lu, G.S. Luo, Chem. Eng. J. 173 (2011) 226–232.
[11] E. Santacesaria, M.D. Serio, P. Iengo, Catal. Today 52 (1999) 363–376.
[12] E. Santacesaria, M.D. Serio, A. Russo, U. Leone, R. Velotti, Chem. Eng. Sci. 54 (1999) 2799–2806.
[13] N. Cherkasov, A.J. Expósito, M.S. Aw, J. Fernández-García, S. Huband, J. Sloan, L. Paniwnyk, E.V. Rebrov, Appl. Catal. A Gen. 570 (2019) 183–191.
[14] P. Insorn, B. Kitiyanan, Catal. Today 256 (2015) 223–230.
[15] A. Drelinkiewicz, A. Waksmundzka-Góra, J.W. Sobczak, J. Stejskal, Appl. Catal. A Gen. 333 (2007) 219–228.
[16] X. Li, H. Su, D. Li, H. Chen, X. Yang, S. Wang, Appl. Catal. A Gen. 528 (2016) 168–174.
[17] Q. Ma, N. Wang, G. Liu, L. Wang, Microporous Mesoporous Mater. 279 (2019) 245–251.
[18] E. Yuan, C. Wu, X. Hou, M. Dou, G. Liu, G. Li, L. Wang, J. Catal. 347 (2017) 79–88.
[19] J.-T. Feng, H.-Y. Wang, D.G. Evans, X. Duan, D.-Q. Li, Appl. Catal. A Gen. 382 (2010) 240–245.
[20] A. Rodríguez-Gómez, F. Platero, A. Caballero, G. Colón, Mol. Catal. 445 (2018) 142–151.
[21] E. Yuan, C. Wu, G. Liu, G. Li, L. Wang, J. Ind. Eng. Chem. 66 (2018) 158–167.
[22] C. Miao, T. Hui, Y. Liu, J. Feng, D. Li, J. Catal. 370 (2019) 107–117.
[23] E. Yuan, C. Wu, G. Liu, L. Wang, Appl. Catal. A Gen. 525 (2016) 119–127.
[24] H. Bai, X. Fang, C. Peng, ACS Sustain. Chem. Eng. 7 (2019) 7700–7707.
[25] J. Zhang, K. Gao, S. Wang, W. Li, Y. Han, RSC Adv. 7 (2017) 6447–6456.
[26] M. Tang, S. Mao, M. Li, Z. Wei, F. Xu, H. Li, Y. Wang, ACS Catal. 5 (2015) 3100–3107.
[27] A. Li, Y.-h. Wang, J. Ren, J.-l. Zhang, W. Li, C.-l. Guo, Appl. Catal. A Gen. 593 (2020), 117422.
[28] S. Fu, H. Zhou, H. Wang, J. Ding, S. Liu, Y. Zhao, H. Niu, G.C. Rutledge, T. Lin, RSC Adv. 8 (2018) 717–723.
[29] C. Zhang, J. Su, H. Zhu, J. Xiong, X. Liu, D. Li, Y. Chen, Y. Li, RSC Adv. 7 (2017) 34182–34191.
[30] N. Hellgren, J. Guo, Y. Luo, C. Såthe, A. Agui, S. Kashtanov, J. Nordgren, H. Ågren, J.-E. Sundgren, Thin Solid Films 471 (2005) 19–34.
[31] H. He, X. Hou, B. Ma, L. Zhuang, C. Li, S. He, S. Chen, Cellulose 23 (2016) 2539–2548.

[32] F. Menegazzo, M. Signoretto, G. Frison, F. Pinna, G. Strukul, M. Manzoli, F. Boccuzzi, J. Catal. 290 (2012) 143–150.
[33] A. Drelinkiewicz, A. Waksmundzka-Góra, W. Makowski, J. Stejskal, Catal. Commun. 6 (2005) 347–356.
[34] K. Pattamakomsan, K. Suriye, S. Dokjampa, N. Mongkolsiri, P. Praserthdam, J. Panpranot, Catal. Commun. 11 (2010) 311–316.
[35] R. Kosydar, A. Drelinkiewicz, E. Lalik, J. Gurgul, Appl. Catal. A Gen. 402 (2011) 121–131.
[36] G. Bombi, S. Lora, M. Zancato, A.A. D'Archivio, K. Jerabek, B. Corain, J. Mol. Catal. A Chem. 194 (2003) 273–281.